

RESEARCH

Open Access



Prediction of hepatocellular carcinoma response to transarterial chemoembolization with intravoxel incoherent motion diffusion-weighted imaging

Abdolkarim Haji Ghadery^{1†}, Niloofar Ayoobi Yazdi^{2†}, Hamed Bagheri³, Anahita Fathi Kazerooni^{4,5}, Faeze Salahshour², Sam Sharifzadeh Javidi^{4,5}, Sandra Saeedi⁶, Hamidreza Saligheh Rad^{4,5†} and Babak Shekarchi^{1*†}

Abstract

Background: There are several therapeutic options for hepatocellular carcinoma (HCC). As predicting the treatment response is critical in clinical decision making, we aimed to evaluate the quantitative intravoxel incoherent motion (IVIM) diffusion-weighted imaging (DWI) parameters as potential predictors of treatment response of HCC lesions to transarterial chemoembolization (TACE).

Results: Twelve patients (eight males; mean age, 56.12 ± 7.88) with 26 confirmed HCC lesions were recruited in the study. Thirteen lesions (50%) responded to TACE, and the remaining lesions were categorized as nonresponder. Age > 60 year (p value: 0.018), D (p value: 0.005), D* (p value: 0.005), and f (p value: 0.004) values were significantly different in response and nonresponse group lesions. Logistic multivariate analysis showed that f value (OR: 0.847 (95% CI 0.732–0.98), p value = 0.025) could independently predict tumor response to TACE. The ROC curve analysis showed f value could predict the HCC response to TACE with sensitivity and specificity of 76.9% and 76.9%, respectively.

Conclusions: IVIM-DWI parameters, especially the f value, might be useful for predicting the response of the intermediate-stage HCC to TACE.

Keywords: Diffusion weighted imaging, Intravoxel incoherent motion, Hepatocellular carcinoma, Transarterial chemoembolization, Treatment response

Background

Primary liver cancer is the sixth most prevalent malignancy worldwide and the third leading cause of cancer mortality. Hepatocellular carcinoma (HCC) is the most common type of liver cancer, accounting for 75–95% of

all primary liver cancer [1]. Due to the asymptomatic feature of HCC, most patients are diagnosed at a late stage and are featured by large and unresectable lesions [2]. Guided by the Barcelona Clinic Liver Cancer (BCLC) classification system, transarterial chemoembolization (TACE) is the first line of treatment for intermediate-stage (stage B) HCC, including unresectable multinodular HCC without extrahepatic spread [3]. TACE has been previously reported to be an efficient bridging therapy for patients waiting for liver transplantation and can improve the survival of inoperable HCC patients [4, 5]. As HCC recurs in up to 70% of cirrhotic patients within

[†]Babak Shekarchi and Hamidreza Saligheh Rad are joint senior authors. Abdolkarim Haji Ghadery and Niloofar Ayoobi Yazdi are joint first authors.

*Correspondence: Shekarchi.babak@yahoo.com

¹ Department of Radiology, AJA University of Medical Sciences, Shahid Etemadzadeh Av., West Fatemi St., P.O. Box 14117-18541, Tehran, Iran
Full list of author information is available at the end of the article

five years after surgery or ablation [6, 7], assessment of tumor recurrence after TACE is crucial for determining treatment success or guiding for subsequent therapeutic planning. Although the BLCL staging system has been helpful in the prognosis of patients [8], a wide range of HCC patients' survival with the BLCL staging system [9] has raised the need for a better or improved predictive model for choosing the best treatment option.

Previous prediction models to estimate the risk of recurrence after treatment were based on qualitative preoperative magnetic resonance imaging (MRI) parameters, including rim enhancement, peritumoral parenchymal enhancement, tumor size, and presence of satellite nodules [10]; however, these indices were mostly subjective which made it difficult to duplicate or promote. Later studies acquired quantitative MRI (qMRI) techniques to provide more information on molecular and metabolism basis of study with intravoxel incoherent motion (IVIM) and diffusion weight imaging (DWI) [11] or Dynamic Contrast-Enhanced MRI [12].

IVIM-DWI has been previously applied to evaluate the prognosis and therapeutic efficacy of different malignant tumors [13–15]. DWI can measure the apparent mobility of water molecules in tissues. The diffusion of water can reflect tissue cellularity, fluid viscosity, and cell membranes [16], which is indicated as apparent diffusion coefficient (ADC) [17]. On the other hand, IVIM values derived from DWI with multiple b value models can reflect tissue diffusion and micro-capillary perfusion separately [18]. Herein, we decided to determine whether IVIM-DWI derived parameters can be used to predict the tumor response to TACE.

Methods:

Ethics

This prospective single-center cohort was approved by our hospital's institutional review board and followed the ethical guidelines of the Declaration of Helsinki. Written informed consent was obtained from each patient before inclusion.

Study population

This study was conducted from February 2019 to January 2020. Fourteen patients with diagnosed HCC, according to the BCLC classification system, were enrolled initially and underwent pretreatment MRI examinations. Inclusion criteria were as follows (1) previously untreated tumor, (2) BCLC stage B tumor without vascular invasion and extrahepatic spread, (3) Child–Pugh grade A or B liver disease, (4) no contraindication for MRI examinations, who were candidates TACE palliative or bridging therapy. Exclusion criteria consisted of (1) glomerular filtration rate < 60, (2) Child–Pugh grade C, (3)

total bilirubin > 4.0 mg/dL, (4) platelet count < 50,000/mL, (5) serum creatinine > 2.0 mg/dL. Two patients were excluded because of limited diffusion imaging quality, rendering interpretation impossible. Post-treatment MRI (30–45 days) scanning was evaluated based on modified Response Evaluation Criteria in Solid Tumors (mRECIST) [19]. Patients with stable disease (SD) or progressive disease (PD) were classified into the nonresponse group, and patients with partial response (PR) or complete response (CR) were classified into the response group.

MRI technique

MRI investigations were performed on a 3.0 T scanner (GE-DISCOVERY MR750W; GE Healthcare) using a commercially available phased array body coil. All patients had fasted for at least 4–6 h before examination and coached on breathing and breath-holding techniques. Conventional MR imaging protocols included breath-hold 2D spin-echo (SE) T1-weighted sequence (TE/TR: 109 ms/4.2 ms, flip angle (FA): 90°, field of view (FOV): 252 × 325 mm, slice thickness: 5 mm, slice gap: 1 mm). T2-weighted GRE sequence (2D multi-echo fast GRE, TE/TR: 47.7 ms/1.4 ms, FA: 25°, FOV: 296 × 3040, matrix size: 128 × 128, slice thickness: 8 mm, slice gap: 1 mm) sequences with breath-hold. The diffusion-weighted imaging was performed by using a respiratory triggered single-shot SE echo-planar imaging (EPI) sequence in the transverse plane. Fifteen b values from 0 to 1500 s/mm² (0, 10, 20, 30, 40, 50, 70, 90, 100, 120, 150, 500, 600, 1000, and 1500) were applied. The acquisition parameters of DWI sequences were as follows: FA: 90°, FOV: 192 × 160 mm, TR /TE: 5000–12,000/73 ms, number of slices: 14, slice thickness: 7 mm, slice gap: 1 mm.

TACE treatment

Patients received TACE from two interventional radiologists with 15 and 20 years of experience. Angiography was performed by femoral artery puncture, and the catheter advanced to celiac artery, which was further placed in the tumor-feeding arteries through selective access of the catheter into the feeding artery. Once the catheter was accurately positioned, an angiogram was used to visualize the tumor. Then, an emulsion consisting of doxorubicin (60 mg), mitomycin (6 mg), and lipiodol (80 mg) was delivered into the catheter and released inside the feeder artery. After surgery, the catheters were pulled out, followed by local compression and pressure bandaging.

Quantification of MR images

The ADC values were estimated by fitting diffusion-weighted signals at all b values (0–1500 s/mm²) to the following mono-exponential equation:

$$\frac{S_b}{S_0} = \exp(-b \cdot ADC)$$

where S_b is the signal intensity at a given b value, and S_0 is the signal intensity without diffusion weighting. Diffusion signal is affected by blood flow in the capillary network and cerebrospinal fluids at low b values (i.e., less than 100–200 s/mm²). Here to calculate coefficients of diffusion, a bi-exponential IVIM quantification model was used as follows [18]:

$$\frac{S_b}{S_0} = (1 - f) \cdot \exp(-b \cdot D) + f \cdot \exp(-b \cdot D^*)$$

where S_0 is the signal at b value of zero, f (fraction of perfusion) is the percentage of a voxel volume occupied by capillaries, D (true diffusion coefficient) is the diffusion parameter representing pure molecular diffusion (“1- f ” reflects the extravascular space where only diffusion effects), and D^* (pseudo-diffusion coefficient) is the proportion of the pseudo-diffusion and reflects dephasing due to perfusion in semi-randomly organized capillaries.

A board-certified abdominal radiologist, who was blinded to all clinical, laboratory, and follow-up information, delineated the regions of interest (ROIs) on the HCC lesions. Borders were drawn along the edge of the tumor on the original images of the DWI sequences by referring to the conventional T1- and T2-weighted images. Tumor size was defined as the maximum diameter of each lesion. The ROIs were automatically copied to the ADC and IVIM maps to obtain the mean apparent diffusion coefficient (ADC), true molecular diffusion coefficient (D), pseudo-diffusion coefficient (D^*), and perfusion fraction (f) values

for each ROI. For each parameter, the average value of all ROIs was calculated.

Statistical analysis

We performed analyses in SPSS (Windows ver. 18; IBM SPSS Inc.) Descriptive data are presented in mean \pm SD / frequency and percentage. We evaluated data normality by Kolmogorov–Smirnov test. We acquired an Independent sample t test for continuous variables with normal distribution, Mann–Whitney U test for continuous non-normal, and Chi-square test for nominal variables. Univariate and multivariate logistic regression analyses were used to identify independent factors for tumor response to TACE in the response group. The final prediction model was derived from the multivariate (backward stepwise) logistic regression analysis results. To define optimum cutoff values for most significant parameters for tumor response to TACE, receiver-operating characteristic (ROC) curves were drawn, and Youden's J index [20] was used. All p values less than 0.05 were considered statistically significant.

Results

Patient's and lesion's baseline characteristics

Twelve patients with HCC (eight males (66.6%); mean age, 56.12 \pm 7.88 years; range, 48–69 years) met the inclusion criteria. In total, 26 lesions (13 in male patients) were included in this study. After TACE, 13 lesions classified in response group (6 lesions (23.1%) with CR, 7 lesions (26.9%) with PR) and 13 classified in nonresponse group (12 lesions (46.2%) with SD, and 1 lesion (3.8%) with PD). All the patients received TACE at least once, and six patients underwent a second TACE following the first treatment. Baseline characteristics of treated Lesions are summarized in (Table 1).

Table 1 Characteristics of HCC Lesions and Their Response to TACE

Variables	All lesions (N = 26)	Response group (N = 13)	Nonresponse group (N = 13)
Gender (male/female)	13/13	9/4	4/9
Age (years)			
≤ 60	12/26	9	3
> 60	14/26	4	10
mean \pm SD	62.3 \pm 11.74	54.85 \pm 7.36	69.92 \pm 10.49
Involved liver lobe (right/left)	13/13	9/4	4/9
Tumor size before TACE (mm)	52.27 \pm 33.95	51.31 \pm 31.87	53.23 \pm 37.2
Tumor size after TACE (mm)	39.12 \pm 33.3	23.77 \pm 21.6	54.46 \pm 36.52

All quantitative values are expressed as mean \pm standard deviation

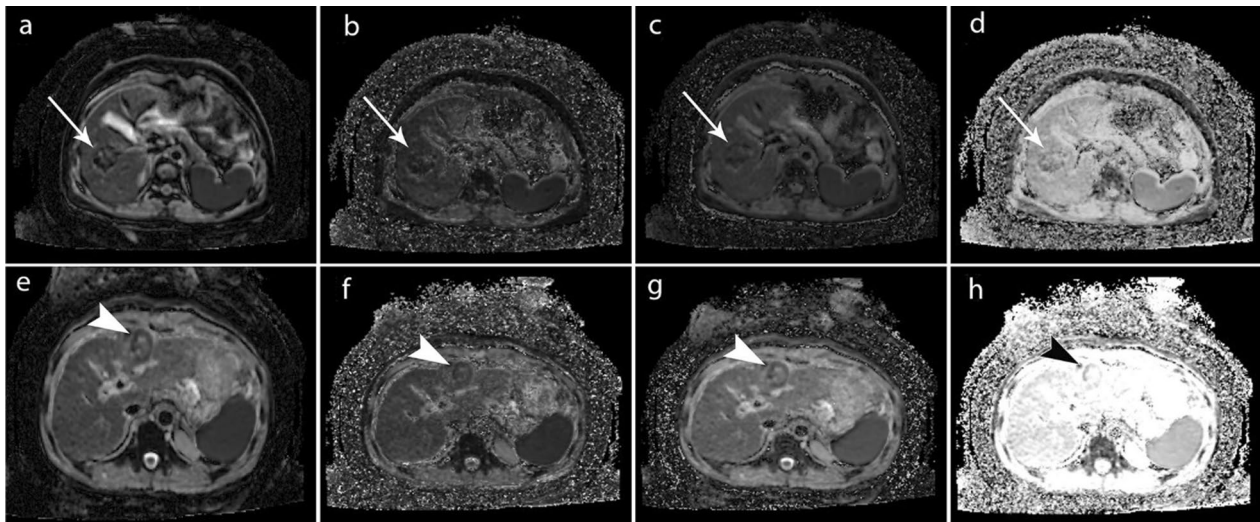


Fig. 1 Pretreatment MR images of two patients with responded and nonresponded lesions to TACE. **a–d** Pretreatment MR Images on the same slice of one lesion in segment eight and right lobe of the liver in a 40-year-old woman who did show tumor response to TACE. **a–d** IVIM-ADC, D, D*, and f maps, with the arrow showing the HCC lesion on the same slice with mean ADC, D, D*, and f values of $0.92 \times 10^{-3} \text{ mm}^2/\text{s}$, $1.04 \times 10^{-3} \text{ mm}^2/\text{s}$, $0.97 \times 10^{-3} \text{ mm}^2/\text{s}$, and $3.53 \times 10^{-3} \text{ mm}^2/\text{s}$, respectively. **e–h** Pretreatment MR Images on the same slice of one lesion in segment four and right lobe of the liver in a 40-year-old man who did not show tumor response to TACE. **e–h** IVIM-ADC, D, D*, f maps, with the arrowhead showing the HCC lesion on the same slice with mean ADC, D, D*, and f values of $0.9 \times 10^{-3} \text{ mm}^2/\text{s}$, $1.23 \times 10^{-3} \text{ mm}^2/\text{s}$, $1.4 \times 10^{-3} \text{ mm}^2/\text{s}$, and $3.9 \times 10^{-3} \text{ mm}^2/\text{s}$, respectively

Differences of qualitative and quantitative parameters between response and nonresponse group

Figure 1 shows pretreatment quantitative MR images for a patient with tumor response and a patient without response to TACE, respectively. There were no significant differences in gender, involved lobe of the liver, ADC, and pre-TACE tumor size between response and nonresponse group (All p values ≥ 0.05). However, age > 60 (p value = 0.018) had a significant difference between two groups. D of tumor tissue in response group ($[-1.45 \pm 4.87] \times 10^{-3} \text{ mm}^2/\text{s}$) was significantly higher

than nonresponse group ($[-7.38 \pm 4.96] \times 10^{-3} \text{ mm}^2/\text{s}$) (p value = 0.005). D* of tumor tissue in response group ($[-1.51 \pm 4.83] \times 10^{-3} \text{ mm}^2/\text{s}$) was also significantly higher than nonresponse group ($[-7.41 \pm 4.91] \times 10^{-3} \text{ mm}^2/\text{s}$) (p value = 0.005). Meanwhile, f value of HCC tumor was significantly higher in response group ($[0.51 \pm 6]$) than nonresponse group ($[-6.9 \pm 5.89]$) (p value = 0.004*) (Table 2).

Table 2 Comparison of baseline and IVIM-DWI parameters between response and nonresponse groups

Variable	Response group	Nonresponse group	p value
Gender (male)	9 (34.61%)	4 (15.38%)	0.05 ^a
Age > 60	4 (15.38%)	10 (38.46%)	0.018 ^a
Lobe of liver (right)	9 (34.61%)	4 (15.38%)	0.05 ^a
ADC ($\times 10^{-3} \text{ mm}^2/\text{s}$)	1.09 ± 0.41	0.89 ± 0.4	0.22
D ($\times 10^{-3} \text{ mm}^2/\text{s}$)	-1.45 ± 4.87	-7.38 ± 4.96	0.005*
D* ($\times 10^{-3} \text{ mm}^2/\text{s}$)	-1.51 ± 4.83	-7.41 ± 4.91	0.005*
f (%)	0.51 ± 6	-6.9 ± 5.89	0.004*
Tumor size before TACE (mm)	51.31 ± 31.87	53.23 ± 37.2	0.88

All quantitative data are expressed as mean \pm standard deviation, all other variables reported as N (%)

ADC apparent diffusion coefficient

*Statistically significant (p value < 0.05)

^a Chi-squared test is used; independent t test or Mann–Whitney U test used for all other comparisons

Tumor response prediction model

As shown in (Table 3), univariate analysis identified that the age > 60, D, D*, and f values of tumor (p values = 0.024, 0.011, 0.010, and 0.009, respectively) acted as independent predictors for tumor response to TACE. In multivariate analysis, f (OR: 0.847 (95% CI 0.732–0.98), p value = 0.025) of tumor tissue was identified as independent predictors for tumor response to TACE.

The ROC curve analysis results for the ability of tumor's D, D*, and f to predict tumor response to TACE

are shown in Fig. 2 and listed in (Table 4). The AUC of D, D*, and f of the tumor tissue were 0.716 (95% confidence interval [CI]: 0.504–0.928), 0.716 (95% CI 0.503–0.929), and 0.775 (95% CI 0.584–0.966), respectively. The optimum cutoff point for D, D*, and f values were –4.52, –4.60, and 2.57, respectively.

Table 3 Univariate and Multivariate Analyses of Pretreatment Prediction for Tumor Response to TACE

Variable	Univariate analysis		Multivariate analysis	
	OR (95% CI)	p value	OR (95% CI)	p value
Gender	0.198(0.037–1.045)	0.056	–	–
Age > 60	7.5 (1.307–43.028)	0.024*	6.064(0.824–44.643)	0.77
Lobe	5.062 (0.957–26.776)	0.056	–	–
D ($\times 10 - 3$ mm ² /s)	0.809 (0.687–0.951)	0.011*	–	–
D* ($\times 10 - 3$ mm ² /s)	0.807 (0.685–0.951)	0.010*	–	–
f (%)	0.836 (0.731–0.957)	0.009*	0.847 (0.732–0.98)	0.025*

The multivariate model was adjusted for age at recruitment (> 60 or \leq 60 years)

*Statistically significant (p value < 0.05)

OR = odds ratio; CI = confidence interval

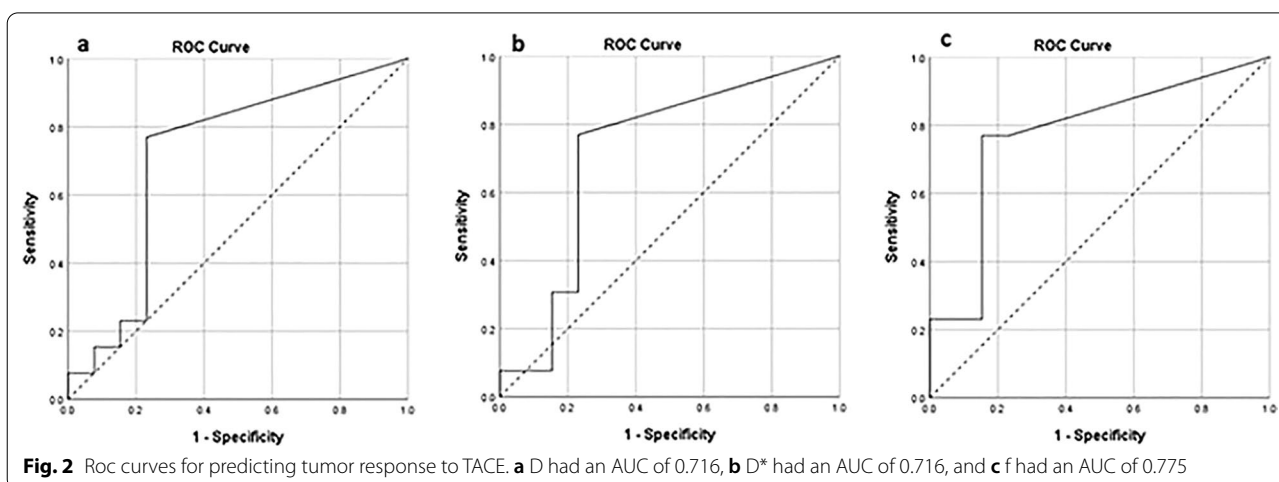


Table 4 Predictive performance for identifying tumor response to TACE

Variable	AUC	p value	Youden's index (%)	Optimum cutoff value	Sensitivity (%)	Specificity (%)	PPV	NPV	Accuracy
D ($\times 10 - 3$ mm ² /s)	0.716 [0.504–0.928]	0.061	0.538	–4.5253	76.92%	76.92%	76.92%	76.92%	76.92%
D* ($\times 10 - 3$ mm ² /s)	0.716 [0.503–0.929]	0.61	0.538	–4.6004	76.92%	76.92%	76.92%	76.92%	76.92%
f (%)	0.775[0.584–0.966]	0.017*	0.615	2.5752	76.92%	76.92%	76.92%	76.92%	76.92%

AUC: areas under the receiver operating characteristic curve, PPV: positive predictive value, NPV: negative predictive value

*Statistically significant (p value < 0.05)

Discussion

Response prediction prior to TACE treatment can help to identify suitable HCC patients. The patients without potential treatment benefits can directly undergo more proper treatment options. Thus, non-beneficial treatments can be delayed until appropriate treatment is available. Therefore, in this study, we tried to find parameters predicting the HCC tumor response to TACE. Our study revealed significant differences in pretreatment IVIM parameters, including D , D^* , and f values, between responding and nonresponding lesions to TACE treatment. Logistic regression analyses showed that the f value of the HCC tumor was an independent predictor for HCC response to TACE.

In the present study, we found that responded lesions to TACE had significantly higher D , D^* , and f values than nonresponded lesions. Similarly, Zhang et al. [21] showed HCC patients with lower preoperative D ($\leq 0.985 \times 10^{-3} \text{ mm}^2/\text{s}$), and f values ($\leq 23.4\%$) tend to have a higher incidence of recurrence. Another study by Jia et al. [11] on Intermediate-Stage Hepatocellular Carcinoma Response to TACE showed pretreatment D of the tumor rather than D^* was significantly different between responded and nonresponded HCC lesions, and D was significantly higher in response group (0.94 ± 0.20) than nonresponse group (0.74 ± 0.22) while D^* and f values were not significantly different in response and non-response group. In line with our findings, a study on the prediction of HCC tumor necrosis based on IVIM parameters by Kakite et al. [22] showed necrotic tumors (1.299 ± 0.250) had significantly higher pretreatment D value compared to viable tumors (1.052 ± 0.231), while D^* and f values were not significantly different among necrotic and viable tumors. IVIM derived parameters can show cell density, microcirculation perfusion, and tissue complexity of lesion [23], and correlation of higher preoperative D , D^* , and f values in our study with tumor response might be due to pathophysiological phenomenon that increased cellular density and nuclear-to-cytoplasmic ratio would be more prominent than blood perfusion when HCC recurs or poorly differentiates [21].

Similar to Jia et al.'s [11] findings, ADC in our study was not significantly different in HCC lesions of responded and nonresponded groups or was not a significant predictor in either univariate or multivariate analysis. However, several studies, until now, investigated ADC value as a predictor of tumor response to locoregional therapies, results are still debated, and some studies have predicted the tumor response with ADC value by defining the specific threshold [24]. For example, Kokabi et al. [25] and Mannelli et al. [26] showed pretreatment ADC value below the threshold ($0.83 \times 10^{-3} \text{ mm}^2/\text{s}$) and above the

threshold ($1.24 \times 10^{-3} \text{ mm}^2/\text{s}$) predicts tumor response, respectively.

Additionally, our analysis showed f value alongside age could independently predict the HCC response to TACE. However, Jia et al. [11] previously reported after multivariate regression, tumor size ($P=0.038$) and APT SI ($P=0.034$) and D ($P=0.038$) of HCC tumor can independently predict the tumor response to TACE.

Our study showed pretreatment IVIM parameters could predict the HCC response to TACE. Regarding the evaluation of every lesion on patients with multiple lesions in the current study, our results might help the clinicians to decide on every lesion in patients with multiple HCC tumors. Regardless of previous quantitative studies on the prediction of HCC response to TACE, with contrast-enhanced MRI, quantitative IVIM-DWI parameters can be utilized when intravenous contrast administration is not possible (in patients with hepatorenal insufficiency) or when small lesions are adjacent to vessels.

Limitations

There were several limitations to the present study. First, our sample size was relatively small. Second, this study was a single-center study, and it is prone to selection bias. Third, our follow-up time was relatively short.

Conclusions

In conclusion, our results suggest that IVIM-DWI quantitative parameters including D , D^* , and f values are associated with HCC lesions response to TACE, and f value can be used as an independent predictor of tumor response to TACE. However, more studies would be needed to make a definite predictive tool based on IVIM-DWI imaging.

Abbreviations

HCC: Hepatocellular carcinoma; BCLC: Barcelona Clinic Liver Cancer; TACE: Transarterial chemoembolization; MRI: Magnetic resonance imaging; qMRI: Quantitative MRI; IVIM: Intravoxel incoherent motion; DWI: Diffusion weight imaging; ADC: Apparent diffusion coefficient; mRECIST: Modified Response Evaluation Criteria in Solid Tumors; SD: Stable disease; PD: Progressive disease; PR: Partial response; CR: Complete response; SE: Spin-echo; FA: Flip angle; FOV: Field of view; EPI: Echo-planar imaging; ROIs: Regions of interest.

Acknowledgements

The authors would like to thank all participants in this study.

Author contributions

AHG was involved in formal analysis, writing—original draft, project administration, NAY helped in conceptualization, investigation, HB contributed to resources, methodology, AFK was involved in software, validation, FS helped in resources, investigation, SSJ contributed to software, validation, SS was involved in resources, methodology, HSR helped in conceptualization, methodology, supervision BS contributed to supervision, investigation. All authors

contributed in writing—review and editing and approved the final version of the manuscript to be published. All authors read and approved the final manuscript.

Funding

This research did not receive any specific grant from funding agencies in the public, commercial, or not-for-profit sectors.

Availability of data and materials

The data that support the findings of this study are not publicly available but will be available from corresponding authors BS Babak Shekarchi or Hamidreza Saligheh Rad upon reasonable request.

Declarations

Ethics approval and consent to participate

This study was performed in line with the principles of the Declaration of Helsinki. Study protocols and patient consent forms were reviewed and approved by the ethics committee of AJA University of Medical Sciences (approval code: IR.AJAUMS.REC.1399.265). All patients signed an informed consent form before entering the study.

Consent for publication

Not applicable.

Competing interests

The authors declare that they have no competing interests.

Author details

¹Department of Radiology, AJA University of Medical Sciences, Shahid Etemadzadeh Av., West Fatemi St., P.O. Box 14117-18541, Tehran, Iran.

²Advanced Diagnostic and Interventional Radiology Research Center, Medical Imaging Center, Tehran University of Medical Sciences, Tehran, Iran. ³Radiation Sciences Research Center (RSRC), AJA University of Medical Sciences, Tehran, Iran. ⁴Department of Medical Physics and Biomedical Engineering, Tehran University of Medical Sciences, Tehran, Iran. ⁵Quantitative Medical Imaging Systems Group (QMISG) Research Center for Molecular and Cellular Imaging, Tehran University of Medical Sciences, Tehran, Iran. ⁶Department of Gastroenterology and Hepatology, AJA University of Medical Sciences, Tehran, Iran.

Received: 11 January 2022 Accepted: 30 March 2022

Published online: 13 May 2022

References

- Sung H, Ferlay J, Siegel RL, Laversanne M, Soerjomataram I, Jemal A et al (2021) Global cancer statistics 2020: GLOBOCAN estimates of incidence and mortality worldwide for 36 cancers in 185 countries. *CA Cancer J Clin* 71(3):209–249
- Chen Q, Cheng C, Chen H, Ning Z, Tang S, Zhang X et al (2014) Effectiveness and complications of ultrasound guided fine needle aspiration for primary liver cancer in a Chinese population with serum α -fetoprotein levels ≤ 200 ng/ml—a study based on 4,312 patients. *PLoS ONE* 9(8):e101536
- Raoul J-L, Forner A, Bolondi L, Cheung TT, Kloeckner R, de Baere T (2019) Updated use of TACE for hepatocellular carcinoma treatment: How and when to use it based on clinical evidence. *Cancer Treat Rev* 72:28–36
- Sapisochin G, Barry A, Doherty M, Fischer S, Goldaracena N, Rosales R et al (2017) Stereotactic body radiotherapy vs. TACE or RFA as a bridge to transplant in patients with hepatocellular carcinoma. An intention-to-treat analysis. *J Hepatol* 67(1):92–99
- Sieghart W, Huckle F, Peck-Radosavljevic M (2015) Transarterial chemoembolization: modalities, indication, and patient selection. *J Hepatol* 62(5):1187–1195
- Poon RT-P, Fan ST, Lo CM, Liu CL, Wong J. Long-term survival and pattern of recurrence after resection of small hepatocellular carcinoma in patients with preserved liver function: implications for a strategy of salvage transplantation. *Annals of surgery*. 2002;235(3):373.
- Tabrizian P, Jibara G, Shrager B, Schwartz M, Roayaie S (2015) Recurrence of hepatocellular cancer after resection: patterns, treatments, and prognosis. *Ann Surg* 261(5):947–955
- Tsilimigras DI, Bagante F, Sahara K, Moris D, Hyer JM, Wu L et al (2019) Prognosis after resection of Barcelona Clinic Liver Cancer (BCLC) stage 0, A, and B hepatocellular carcinoma: a comprehensive assessment of the current BCLC classification. *Ann Surg Oncol* 26(11):3693–3700
- Pinato DJ, Howell J, Ramaswami R, Sharma R (2017) delivering precision oncology in intermediate-stage liver cancer. *Aliment Pharmacol Ther* 45(12):1514–1523
- An C, Kim DW, Park Y-N, Chung YE, Rhee H, Kim M-J (2015) Single hepatocellular carcinoma: preoperative MR imaging to predict early recurrence after curative resection. *Radiology* 276(2):433–443
- Jia F, Wu B, Yan R, Li L, Wang K, Han D (2020) Prediction model for intermediate-stage hepatocellular carcinoma response to transarterial chemoembolization. *J Magn Reson Imaging* 52(6):1657–1667
- Hsu C-Y, Shen Y-C, Yu C-W, Hsu C, Hu F-C, Hsu C-H et al (2011) Dynamic contrast-enhanced magnetic resonance imaging biomarkers predict survival and response in hepatocellular carcinoma patients treated with sorafenib and metronomic tegafur/uracil. *J Hepatol* 55(4):858–865
- Niu J, Li W, Wang H, Wu W, Gong T, Huang N et al (2017) Intravoxel incoherent motion diffusion-weighted imaging of bone marrow in patients with acute myeloid leukemia: a pilot study of prognostic value. *J Magn Reson Imaging* 46(2):476–482
- Zhu L, Wang H, Zhu L, Meng J, Xu Y, Liu B et al (2017) Predictive and prognostic value of intravoxel incoherent motion (IVIM) MR imaging in patients with advanced cervical cancers undergoing concurrent chemoradiotherapy. *Sci Rep* 7(1):1–9
- Messina C, Bignone R, Bruno A, Bruno F, Calandri M et al (2020) Diffusion-weighted imaging in oncology: an update. *Cancers* 12(6):1493
- Koh D-M, Collins DJ (2007) Diffusion-weighted MRI in the body: applications and challenges in oncology. *Am J Roentgenol* 188(6):1622–1635
- Barral M, Taouli B, Guiu B, Koh D-M, Luciani A, Manfredi R et al (2015) Diffusion-weighted MR imaging of the pancreas: current status and recommendations. *Radiology* 274(1):45–63
- Le Bihan D, Breton E, Lallemand D, Aubin M, Vignaud J, Laval-Jeantet M (1988) Separation of diffusion and perfusion in intravoxel incoherent motion MR imaging. *Radiology* 168(2):497–505
- Lencioni R, Llovet JM, editors. Modified RECIST (mRECIST) assessment for hepatocellular carcinoma. *Seminars in liver disease*; 2010: © Thieme Medical Publishers.
- Youden WJ (1950) Index for rating diagnostic tests. *Cancer* 3(1):32–35
- Zhang Y, Kuang S, Shan Q, Rong D, Zhang Z, Yang H et al (2019) Can IVIM help predict HCC recurrence after hepatectomy? *Eur Radiol* 29(11):5791–5803
- Kakite S, Dyvorne HA, Lee KM, Jajamovich GH, Knight-Greenfield A, Taouli B (2016) Hepatocellular carcinoma: IVIM diffusion quantification for prediction of tumor necrosis compared to enhancement ratios. *Eur J Radiol Open* 3:1–7
- Park YS, Lee CH, Kim JH, Kim IS, Kiefer B, Seo TS et al (2014) Using intravoxel incoherent motion (IVIM) MR imaging to predict lipiodol uptake in patients with hepatocellular carcinoma following transcatheter arterial chemoembolization: a preliminary result. *Magn Reson Imaging* 32(6):638–646
- Ludwig JM, Camacho JC, Kokabi N, Xing M, Kim HS (2015) The role of diffusion-weighted imaging (DWI) in locoregional therapy outcome prediction and response assessment for hepatocellular carcinoma (HCC): the new era of functional imaging biomarkers. *Diagnostics* 5(4):546–563
- Kokabi N, Ludwig JM, Camacho JC, Xing M, Mittal PK, Kim HS (2015) Baseline and early MR apparent diffusion coefficient quantification as a predictor of response of unresectable hepatocellular carcinoma to doxorubicin drug-eluting bead chemoembolization. *J Vasc Interv Radiol* 26(12):1777–1786
- Mannelli L, Kim S, Hajdu CH, Babb JS, Taouli B (2013) Serial diffusion-weighted MRI in patients with hepatocellular carcinoma: prediction and assessment of response to transarterial chemoembolization. *Prelim Exp Eur J Radiol* 82(4):577–582

Publisher's Note

Springer Nature remains neutral with regard to jurisdictional claims in published maps and institutional affiliations.

Submit your manuscript to a SpringerOpen[®] journal and benefit from:

- Convenient online submission
- Rigorous peer review
- Open access: articles freely available online
- High visibility within the field
- Retaining the copyright to your article

Submit your next manuscript at ► [springeropen.com](https://www.springeropen.com)
